Comparison of Methods for Horizon Line Detection in Sea Images

Tzvika Libe, Evgeny Gershikov and Samuel Kosolapov
Department of Electrical Engineering
Braude Academic College of Engineering
Karmiel 21982, Israel
e-mail: tzvika_libe1@walla.com , eugeny11@braude.ac.il (corresponding author) and ksamuel@braude.ac.il

Abstract— **Four algorithms designed to find a horizontal line separating sea from sky in real-life conditions were implemented and compared by their accuracy and relative speed. The algorithms selected were H-COV-LUM, based on regional covariances in luminance images, H-HC, based on edge detection and the Hough transform, H-LSC, based on maximal edge detection and the least squares method and H-MED, based on median filtering and linear regression. Real-life images were used for comparison. The most accurate line with respect to angular error was obtained by using the H-HC algorithm and with respect to the error in the position of the line by H-COV-LUM, whereas the highest speed was achieved by using the H-LSC method.**

Keywords-horizon detection; marine images; edge detection; median filtering; image analysis

I. INTRODUCTION

The horizon line is used for different purposes, such as navigation in airborne and marine vehicles and military surveillance. A number of horizon line detection methods are known [1,2,5,6,7,10,11]. Some of these methods are based on edge detection [9], while others employ different techniques. Due to the variety of techniques, a comparison of the detection performance that they can achieve can be very helpful. The goal of this research is to implement and compare the accuracy of a number of well-known and modified horizon-line detection approaches. Considering that in the later stages of this research the selected algorithm is to be implemented on a stand-alone hardware unit, algorithms complexity and their relative speed is also evaluated.

The structure of this paper is as follows. In the next section we present the algorithms discussed in this work for horizon line detection in marine images. Then in Section III we describe the methods and criteria used in the comparison of these algorithms. Section IV is dedicated to horizon detection results: quantitative and visual and, finally, Section V presents a summary of this work and our conclusions.

II. ALGORITHMS COMPARED

Four algorithms are compared in this work. The motivation for their choice is comparison of local feature based algorithms, such as those based on edges, with global feature based methods, such as H-COV-LUM, that uses regional covariances. The H-MED algorithm extends the meaning of a local feature (edge) at a pixel to its small neighborhood and then looks for the maximal edge in the vertical direction. Thus it introduces a compromise between local and global features. No algorithms that require a training stage, such as neural networks and support vector machines were chosen for the comparison, but only simple low complexity methods were taken.

The compared methods are:

"H-COV-LUM" – an algorithm that uses regional covariances, as introduced in [5], but calculated on luminance images. Although there are cases where the color information is important [8], in this case, using achromatic image data only improves the algorithm speed significantly with minimal loss in accuracy.

"H-HC" – using pre-processing, Canny edge detector [3] and Hough transform [4].

"H-LSC" – using pre-processing, edge detection and calibration by the least-squares method approach.

"H-MED" – seeking for the maximal edge in the vertical direction, followed by median filtration in order to reject outlying points and linear regression.

The algorithms are described in more detail in the next subsections.

A. Regional covariance based algorithm (H-COV-LUM)

An algorithm for horizon detection for remotely piloted Micro Air Vehicles was introduced in [5]. The algorithm receives an image taken from the air as input and searches for an optimal partition of the image into two regions: sky and ground (or sky and sea) using a line, which is the detected horizon. The optimization criterion is based on the determinants and the traces of the covariance matrices of the two regions. More specifically, if we denote a sky pixel by $\boldsymbol{x}^s_{i,j} = [R^s_{i,j}\ \mathrm{G}^s_{i,j}\ \mathrm{B}^s_{i,j}]^T$, where $R^s_{i,j}, \mathrm{G}^s_{i,j}, \mathrm{B}^s_{i,j}$ are the primary red, green and blue values at the pixel (i,j), and we denote a ground pixel by $\boldsymbol{x}^g_{i,j} = [R^g_{i,j}\ G^g_{i,j}\ B^g_{i,j}]^T$, then the covariance matrices of the regions are given by $\Lambda^s = E\left(\left(\boldsymbol{x}^s_{i,j} - \mu^s\right)\left(\boldsymbol{x}^s_{i,j} - \mu^s\right)^T\right)$, $\boldsymbol{\mu}^s = E\left(\boldsymbol{x}^s_{i,j}\right)$ and $\Lambda^g = E\left(\left(\boldsymbol{x}^g_{i,j} - \mu^g\right)\left(\boldsymbol{x}^g_{i,j} - \mu^g\right)^T\right)$, $\boldsymbol{\mu}^g = E\left(\boldsymbol{x}^g_{i,j}\right)$. E() denotes here statistical mean. The optimization criterion, considered for all the possible horizon line orientations and positions and maximized is given by [5]:

$$J = \frac{1}{\det(\Lambda^s) + \det(\Lambda^g) + trace^2(\Lambda^s) + trace^2(\Lambda^g)}, \quad (1)$$

where det() denotes the determinant and trace() denotes the trace of the covariance matrices Λ^s and Λ^g.

We consider a similar criterion to the one in (1) for the luminance image, thus the optimization term J becomes

$$J = \frac{1}{\mathrm{var}(Y^s) + \mathrm{var}(Y^g) + \mathrm{var}^2(Y^s) + \mathrm{var}^2(Y^g)}, \quad (2)$$

where var() stands for variance and Y^s, Y^g are the luminance values of the sky and ground regions, respectively. A simplified optimization criteria

$$J = \frac{1}{\mathrm{var}(Y^s) + \mathrm{var}(Y^g)} \quad (3)$$

can be used instead of the one in (2) with similar results. Also, defining a region of interest (ROI) in the image and searching the horizon line only in this area speeds up the algorithm significantly. Alternatively, the input image can be down-sampled prior to the application of the algorithm to reduce its runtime, but this will decrease the accuracy as well.

B. *Edge detection and Hough transform based algorithm* (H-HC)

The stages of this method can be summarized as follows:

1. Pre-process the image using morphological erosion to reduce the probability of the detection of weak edges in the later stages. A small circular structuring element can be used here. Alternatively, the image can be smoothed using a low pass filter, but we found erosion to provide better performance.
2. Apply Canny [3] edge detector to the pre-processed image.
3. Apply the Hough transform [4] to the edges map.
4. Choose the horizon line to be the longest line found in the previous step.

C. *Edge detection and least squares calibration based algorithm (H-LSC)*

This algorithm is based on edge detection as well, but uses a simple algorithm to detect the maximal vertical edge in each column of the image. Its stages are described below.

1. Pre-process the image using morphological erosion.
2. Find the maximal vertical edge in each column of the image. The simplest way to measure the edge strength is using an approximation of the vertical derivative, e.g., $\left|Y_{i,j} - Y_{i+1,j}\right|$. Store the (i,j) coordinates of the maximal edges.
3. Use the least squares method to find the optimal line passing through the maximal edges' coordinates. Edges with very small values as well as very big ones can be discarded here for better algorithm resilience to noise.

D. *Median filtering and linear regression based algorithm (H-MED)*

This algorithm employs median filters in several stages providing high performance in the presence of noise. The stages of the algorithm are:

1. Pre-process the image using morphological erosion.
2. Find the maximal vertical edge in each column of the image. Here the edge at pixel (*i,j*) is measured as the absolute difference between two median values of the 5 pixels above and including pixel (*i,j*) and the 5 pixels below it, i.e., $edge_{i,j} = \left|med_1 - med_2\right|$, where

$$med_1 = median\left\{Y_{k,j}\right\}_{k=i-4}^{i},$$
$$med_2 = median\left\{Y_{k,j}\right\}_{k=i+1}^{i+5}. \quad (4)$$

and.

The (*i,j*) coordinates of the maximal edges are stored.

3. Use linear regression to find the optimal line passing through the maximal edges' coordinates.
4. An optional step of median filtering can be added to remove outliers. This step can be applied to the vertical coordinates of the maximal edges (prior to Step 3) or to the regression errors (following Step 3). We define the regression error as the error at coordinates (*i,j*) of a maximal edge, i.e.,

$$err_{i,j} = \left|i - a_1 j - a_0\right|, \quad (5)$$

where a_0, a_1 are the optimal line coefficients found in Step 3. We define the median filtered error $err_{i,j}^{med}$ as $err_{i,j}$ after applying a median filter. Now the outliers are (*i,j*), where $\left|err_{i,j} - err_{i,j}^{med}\right| > Th$. Th here is the threshold (e.g., a value of 1).

III. COMPARISON METHODS AND CRITERIA

Next, we describe the images and criteria used for the comparison of the algorithms in this work.

A. *Images used to compare the algorithms*

The results of horizon detection for a group of 9 marine images are presented in this work. Image input format is true color (24 bit per pixel) non-compressed BMP. Resolutions used vary from 249x169 to 900x675 pixels. Most images contain a horizon line separating the sea and the sky clearly distinguished by the human eye. However, sometimes the horizon line is slightly distorted by camera optics and sea waves or concealed by marine vessels. To further challenge the selected algorithms, several images contained clouds or sun light effects near the surface of the sea water.

 ISBN: 978-1-61208-220-2

B. Comparison criteria

The algorithms were compared with respect to accuracy and speed. The accuracy was measured for the detected horizon angle relative to a horizontal line (in degrees) as well as the height of the line above the bottom left corner of the image (in pixels). The errors provided in the next section for these two horizon line parameters are measured relative to the line height and angle as determined visually. The algorithms' speed was measured in terms of run time (in seconds).

IV. RESULTS

The accuracy comparison for the algorithms described above (height and angle deviations) is given in Table 1 in terms of the mean errors for 9 test images. In some of these images the horizon is not horizontally aligned (e.g., see Fig. 1). As it can be seen, the angular deviation is very small on average for the H-LSC and H-HC algorithms. The height deviation is smallest for the H-COV-LUM method, based on regional covariances in luminance images. However, the fastest algorithm is H-LSC, based on maximal edges and least squares optimization, as seen from the run time comparison in Table 2. The H-COV-LUM and H-MED algorithms are significantly slower than H-LSC due to the required computations of regional covariances or local medians in the process of the horizon detection.

Algorithm	Mean height deviation	Mean angle deviation
H-LSC	1.92	0.23 °
H-COV-LUM	1.11	0.47 °
H-HC	1.67	0.13 °
H-MED	1.83	0.44 °

TABLE 1. MEAN HEIGHT DEVIATION (PIXELS) AND ANGLE DEVIATION (DEGREES) FOR THE FOUR ALGORITHMS

Algorithm	Mean Time (sec.)
H-LSC	0.3
H-COV-LUM	2.8
H-HC	0.4
H-MED	2.5

TABLE 2. MEAN RUN TIMES (SECONDS) FOR THE FOUR HORIZON DETECTION ALGORITHMS

A. Visual results

Visual results are provided in Figs. 1, 2 and 3. As it can be seen, all the algorithms provide similar good results for the Horizon_1 image (Fig. 1), although the H-COV-LUM method slightly misses the horizon line. This is due to the effect of the clouds and the sunlight reflection in the sea water. A similar effect can be seen for the Horizon_5 image (Fig. 2), where the H-COV-LUM method provides a slightly less accurate estimate of the horizon line than the other algorithms that achieve visually similar performance with good detection of the horizon. H-COV-LUM is thus an efficient algorithm for locating the position of the center of the horizon line, but sometimes the line is slightly rotated compared to the optimal one introducing an angular error. The algorithm copes well with images where the sky and the sea are uniform in appearance even when marine vessels are present, but it may be confused by clouds, sun reflection effects (Fig. 1) and strong waves (Fig. 2). The solution to this may be a pre-processing stage which removes some of the clouds, light reflection effects and waves from the image resulting in more uniform sky and sea areas. This is currently under research.

In Fig. 3, both H-COV-LUM and H-HC methods provide good estimates of the horizon line, while H-LSC is less accurate. As for H-MED, its performance is inferior to the others due to a bigger angular error. This method is more affected by the closer ship concealing the horizon line. The reason for the performance decrease for H-LSC and H-MED is that both detect maximal edges at pixels of the larger marine vessel instead of the horizon that is partly hidden. Than the least squares technique or the linear regression employed to find the optimal line passing through the maximal edge locations produce a line that is shifted downwards relative to the optimal horizon line. The solution to this problem can be calculating the optimal line many times using partial data and then choosing the one passing through or close to the maximal number of edge pixels. This is currently under research.

The H-HC algorithm, on the other hand, is robust to the hindrances introduced by the sea vessels in the image of Fig. 3 due to the use of the Hough transform that detects the line passing through the maximal number of pixels in the edge map. Thus, even though some of the ship pixels are detected as edges, this does not confuse the method as long as more pixels are marked as edges on the real horizon line.

V. CONCLUSIONS

Four different algorithms for horizon detection in marine images were examined in this work. The techniques employed by these algorithms vary from using regional covariances of sky and sea regions (H-COV) to using edge detection and Hough transform (H-HC), using maximal edge detection and the least squares method (H-LSC) and using median filtering and linear regression (H-MED). The algorithms were implemented and compared for a group of test images with respect to accuracy as well as speed. The most accurate method with respect to the angular error was found to be H-HC, while the other algorithms do not lag far behind. The H-COV algorithm provided the highest accuracy when estimating the height of the horizon line above the bottom left corner of the image. Also when

 ISBN: 978-1-61208-220-2

comparing the algorithms' speed, the fastest method was H-LSC. We conclude that all the algorithms examined in this work can be used for horizon detection in still marine images. Moreover, the algorithms can be used also in images taken by infrared cameras, which is the subject of future research.

ACKNOWLEDGMENT

We would like to thank the administration of Ort Braude college and the Department of Electrical Engineering for providing the opportunity to conduct this research and the financial means to present it at the conference.

REFERENCES

[1] G. Bao, Z. Zhou, S. Xiong, X. Lin, and X. Ye, "Towards micro air vehicle flight autonomy research on the method of horizon extraction", Proc. IEEE Conf. on Instrumentation and Measurement Technology, 2003, vol. 2, pp. 1387-1390.

[2] G.-Q. Bao, S.-S. Xiong, and Z.-Y. Zhou, "Vision-based horizon extraction for micro air vehicle flight control", IEEE Trans. on Instrumentation and Measurement, 54(3), 2005, pp. 1067-1072.

[3] J. Canny, "A computational approach to edge detection", IEEE Transactions on PAMI, 8(6), 1986, pp. 679-697.

[4] R. O. Duda and P. E. Hart, "Use of the Hough Transformation to Detect Lines and Curves in Pictures", Comm. ACM, 15(1), 1972, pp. 11–15.

[5] S. M. Ettinger, M. C. Nechyba, P. G. Ifju, and M. Waszak, "Vision-guided flight stability and control for micro air vehicles", Proc. IEEE Conf. on Intelligent Robots and Systems, Lausanne, Switzerland, 2002, pp. 2134 – 2140.

[6] S. Fefilatyev, V. Smarodzinava, L.O. Hall, and D.B. Goldgof, "Horizon detection using machine learning techniques". Proc. Intern. Conf. on Machine Learning and App., 2006, pp. 17-21.

[7] S. Fefilatyev, D.B. Goldgof, and L. Langebrake. "Towards detection of marine vehicles on horizon from buoy camera". Proc. SPIE, 2007, pp. 6736:67360O.

[8] E. Gershikov and M. Porat, "On color transforms and bit allocation for optimal subband image compression", Signal Processing: Image Communication, 22(1), Jan. 2007, pp. 1-18.

[9] S. Kosolapov, "Robust Algorithms Sequence for Structured Light 3D Scanner Adapted for Human Foot 3D Imaging", Journal of Comm. and Computer, 8(7), 2011, pp. 595-598.

[10] K. Nonami, F. Kendoul, S. Suzuki, W. Wang, and D. Nakazawa, Autonomous flying robots (Springer, Tokyo, Dordrecht, Heidelberg, London, New York, 2010).

[11] Y. Wang, Z. Liao, H. Guo, T. Liu, and Y. Yang, "An Approach for Horizon Extraction in Ocean Observation", Proc. IEEE Congress on Image and Signal Processing, 2009, Tianjin, China, pp. 1-5.

 ISBN: 978-1-61208-220-2

H-COV result for Horizon_1

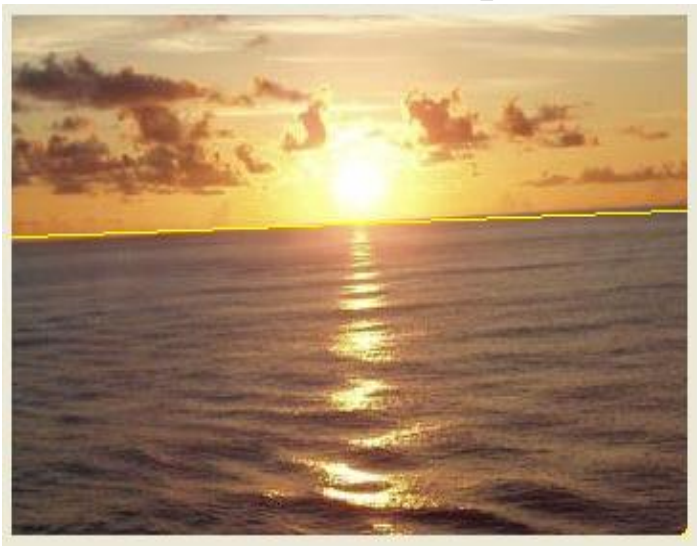

H-LSC result for Horizon_1

H-MED result for Horizon_1

H-HC result for Horizon_1

Figure 1. Horizon detection results for image Horizon_1. The (yellow) line marks the detected horizon. Note the clouds and reflected light effects in this image.

 ISBN: 978-1-61208-220-2

H-COV result for Horizon_5

H-LSC result for Horizon_5

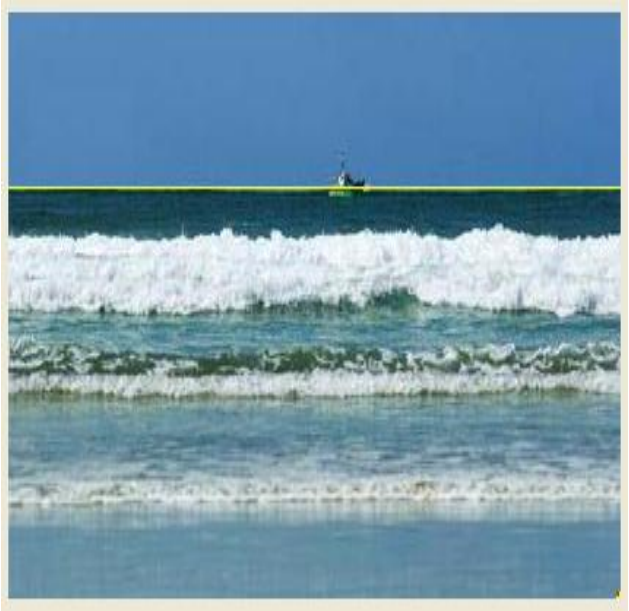

H-MED result for Horizon_5

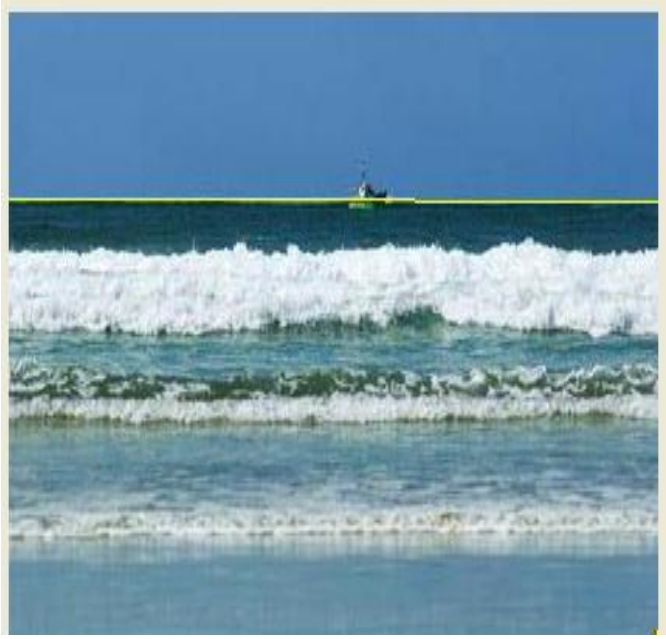

H-HC result for Horizon_5

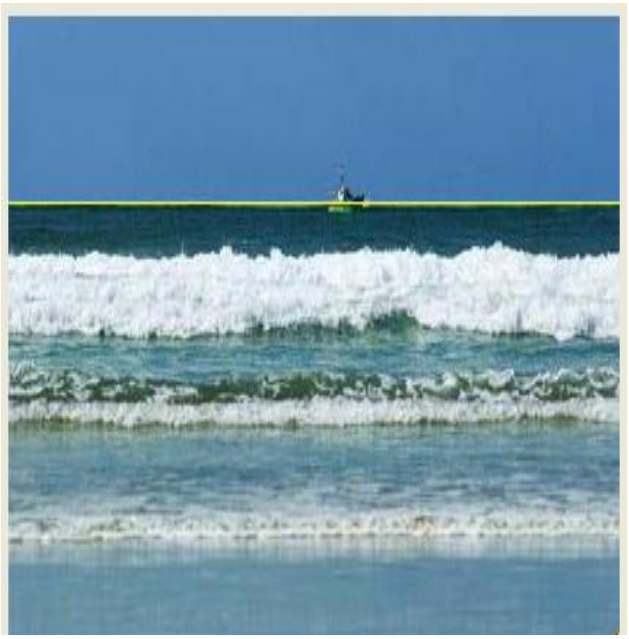

Figure 2. Horizon detection results for image Horizon_5. The (yellow) line marks the detected horizon. Despite the waves and the ship present, all the algorithms detect the horizon correctly.

 ISBN: 978-1-61208-220-2

H-COV result for Horizon_6

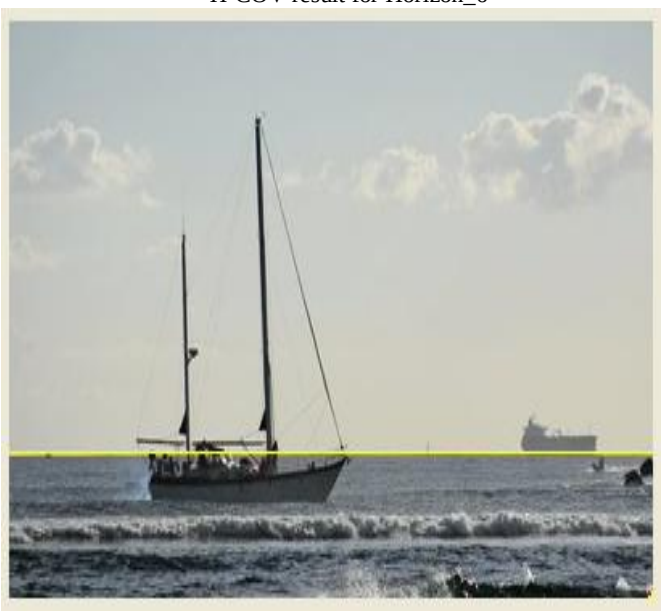

H-LSC result for Horizon_6

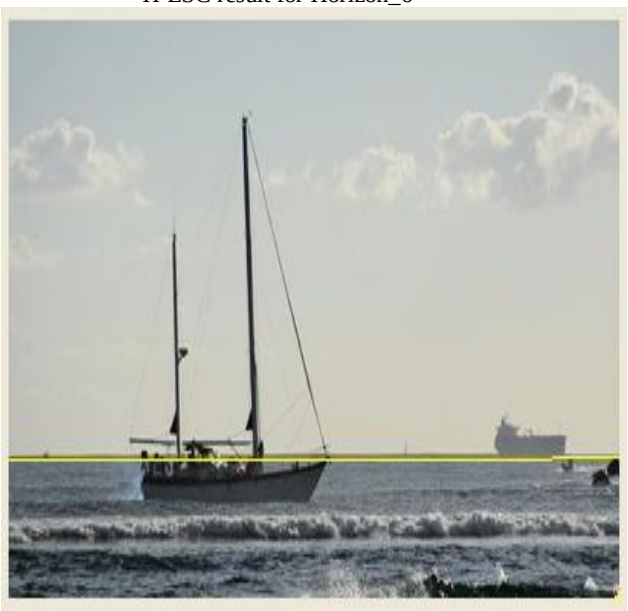

H-MED result for Horizon_6

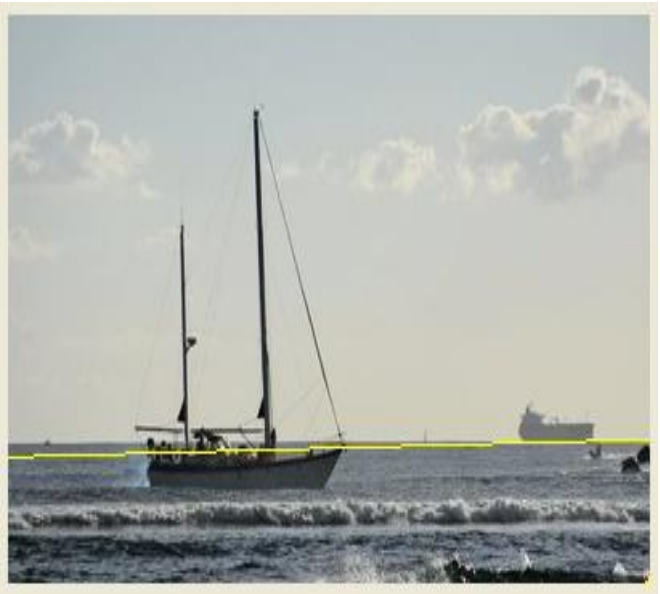

H-HC result for Horizon_6

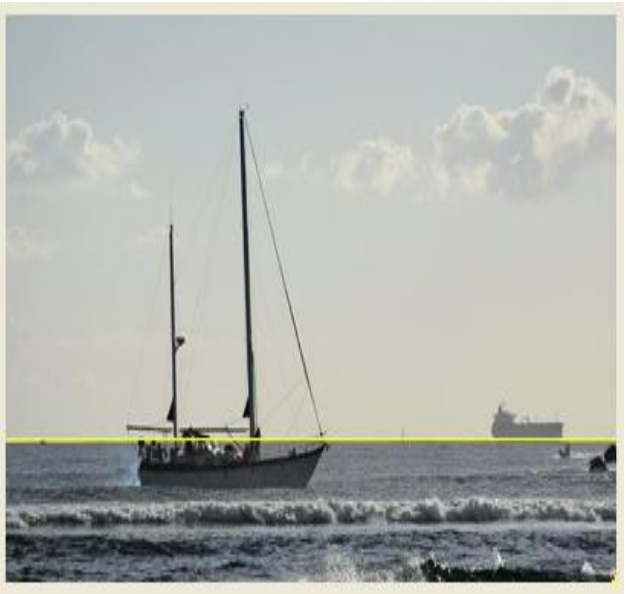

Figure 3. Horizon detection results for image Horizon_6. The (yellow) line marks the detected horizon. Note the waves and the sea vessels present in this image, especially the closer one blocking the horizon.

.

 ISBN: 978-1-61208-220-2